A&A 457, 995–1001 (2006)
DOI: 10.1051/0004-6361:20065481

Astronomy & Astrophysics

Does the oxygen-sodium anticorrelation in globular clusters require a lowering of the ^{23}Na(p,α)^{20}Ne reaction rate?

P. Ventura and F. D'Antona

INAF - Observatory of Rome, via Frascati 33, 00040 MontePorzio Catone (RM) – Italy
e-mail: [ventura;dantona]@oa-roma.inaf.it

Received 24 April 2006 / Accepted 3 July 2006

ABSTRACT

Context. The chemical content of the ejecta of Asymptotic Giant Branch stars (AGBs) is important to understand whether intermediate mass stars played a role in the "self-enrichment scenario", to explain the chemical anomalies observed among Globular Clusters stars. One difficulty of this model is that it is not fully consistent with the observed oxygen-sodium anticorrelation.
Aims. We look for the combinations of the input-physics parameters by which the yields of massive AGBs are sodium-rich and oxygen-poor.
Methods. Many evolutions from the early evolutionary phases until the mass of the envelope drops below ∼0.5 $M_{\odot}$ are calculated for a 5 $M_{\odot}$ $Z = 0.001$ model for various assumptions concerning the extra mixing from the bottom of the envelope and the relevant cross sections involving sodium.
Results. A modest amount of extra mixing from the bottom of the surface convective zone leads to ejecta that are moderately sodium rich and oxygen depleted. A different but appealing modelization allows us to reproduce the observations of stars with a lower oxygen content: extra mixing is not included, but the cross sections of the reaction ^{23}Na$(p,\alpha)^{20}$Ne must be a factor of ∼4 lower than the recommended values. If the initial neon content of the star is not solar-scaled but enhanced as the other α elements by a factor ∼2, the afore mentioned cross section must be lessened by only a factor ∼2.

Key words. stars: abundances – stars: AGB and post-AGB – stars: evolution

1. Introduction

It is well known that stars in Globular Clusters (GCs) are far from representing chemically homogeneous samples. Deep spectroscopic analysis of giants and even Turn Off (TO) stars evidentiated strong differences in the observed chemical compositions, with systematic trends involving the abundances of some key-elements like oxygen, sodium, magnesium, fluorine and aluminum (see e.g. Gratton et al. 2004; Sneden et al. 2004).

The most evident and confirmed among these patterns is the oxygen-sodium anticorrelation, which was observed in all the GCs so far examined (Carretta 2006): along with a "standard" stellar population, made up of sources with [^{23}Na/Fe] ∼ 0 and [^{16}O/Fe] ∼ 0.3[1], a tail of stars with enhanced sodium and depleted oxygen is systematically found. Compared to the trends involving other elements, the oxygen-sodium anticorrelation is particularly interesting due to the large spread of the abundances of both the elements involved: oxygen varies by ∼0.8 dex (reaching 1.5 dex in the peculiar GC M13), and sodium by ∼0.6 dex. The range of values spanned by the oxygen and sodium abundances are such that observational errors cannot be invoked to explain the anomalous behaviour.

The detection of such anomalous patterns in TO stars rules out the possibility that these abundances are fully determined by in situ processes, and shifts the attention towards self-enrichment scenarios (Ventura et al. 2001; Yong et al. 2003; Denissenkov & Weiss 2004; Piotto et al. 2005; D'Antona et al. 2005; Yong et al. 2006). One common interpretation is that the stars with non standard composition were formed within an environment that was polluted by the winds of an early massive AGB population: these stars evolve rapidly (from 50 to ∼100 Myr), and may attain at the bottom of their external convective zone temperatures large enough ($T \sim 10^8$ K) to favour "Hot Bottom Burning" (Blöcker & Schonberner 1991; hereinafter HBB), with the consequent alteration of the surface abundances, due to the rapidity of convective motions. To confirm the validity of this hypothesis it is necessary that the AGB yields are sodium-rich and oxygen-poor[2]. Unfortunately, the chemical content of the ejecta of these stars, as well as the whole physical evolution of AGBs, turns out to be extremely sensitive to all the uncertainties characterizing the input physics (i.e. convection, mass loss, extra mixing, cross sections...) used when calculating the evolutionary models (Ventura & D'Antona 2005a,b); this is the main reason why the yields provided by different groups working on this topic are very different from each other, even by 2 orders of magnitude for sodium.

Ventura et al. (2001) showed that when an efficient treatment of convection is used, it is possible to achieve depletion of oxygen at the bottom of the outer convective zone.

[1] Where we indicate with $[X] = \log X - \log X_{\odot}$.

[2] Apart from the difficulties connected with the reproduction of the observed chemical anomalies in GC stars, discussed in the present paper, there are other problems in the scenario of self-enrichment by AGB winds. In particular, the initial mass function (IMF) of the first stellar generation to which the AGB pollutors belong should have been peculiarly rich in intermediate mass stars, and the efficiency of star formation must have been very high (Cottrell & Da Costa 1981; D'Antona & Caloi 2004). There are several qualitative proposals of scenarios to deal with this problem, but no precise computation of the gas dynamics and of the second generation star formation is yet available.

Ventura & D'Antona (2005a) presented models that, for $M \sim 4-4.5\ M_{\odot}$, showed a mild depletion of oxygen (by ∼0.3 dex) and an enhancement of sodium (by ∼0.4 dex), in agreement with the bulk of the abundances measured in the anomalous population; on the contrary, their massive AGB ($M \geq 5\ M_{\odot}$) models have temperatures so high that sodium is destroyed, providing a negative sodium yield.

In this paper we address the issue of sodium production (or destruction) within massive AGBs, studying in great detail the role played by a possible extra-mixing region below the bottom of the external convective zone, as preliminarily discussed by Ventura & D'Antona (2005c). We also study the role of the cross sections for the proton-capture reactions by ^{22}Ne and ^{23}Na nuclei, which have been considerably revised with respect to the NACRE compilation (Angulo et al. 1999), adopted in our previous works. We focus our attention on a typical massive model characterized by strong HBB (i.e. 5 $M_{\odot}$), to understand if and to which extent its ejecta are consistent with the self-enrichment scenario.

2. The ATON stellar evolution code

The stellar evolution code used in this work is ATON, a full description of which can be found in Ventura et al. (1998). Here we briefly recall the main physics inputs.

2.1. Convection

The thermodynamic description of the regions unstable to convective motions can be addressed either within the context of the traditional Mixing Length Theory (MLT) formulation (Vitense 1953), or by the Full Spectrum of Turbulence (FST) model (Canuto et al. 1996). A detailed description of the differences in the physics of these two formalisms can be found in Canuto & Mazzitelli (1991). All the evolutions presented in this work were calculated by adopting the FST treatment.

2.2. Mixing

Mixing of chemicals within convective zones can be addressed within the instantaneous mixing framework or by a diffusive approach. In this case, for each chemical species a diffusive-like equation (Cloutman & Eoll 1976) is solved:

$$\frac{\mathrm{d}X_i}{\mathrm{d}t} = \left(\frac{\partial X_i}{\partial t}\right)_{\mathrm{nucl}} + \frac{\partial}{\partial m_r}\left[(4\pi r^2\rho)^2 D \frac{\partial X_i}{\partial m_r}\right] \quad (1)$$

where D is the diffusion coefficient, for which a local approximation ($D \sim \frac{1}{3}vl$) is adopted.

The borders of the convective regions are fixed according to the Schwarzschild criterium. It is also possible to consider some extra mixing, by allowing convective velocities to decay exponentially from the formal border, with an e-folding distance described by the free-parameter ζ (see Ventura et al. (1998) for a complete discussion regarding the variation of convective velocities in the proximities of the convective borders). Due to the importance that CNO burning within the most internal part of the convective envelope may have on the AGB evolution, we adopted the diffusive treatment in all the models presented here. During the two major nuclear burning phases in the central regions of the star, an overshooting parameter $\zeta = 0.02$ was adopted, in agreement with the calibration given in Ventura et al. (1998), to describe the exponential decay of velocity from the formal border of the convective core. In most cases no extra mixing from the bottom of the convective envelope before the first thermal pulse (TP) was adopted; the effects of the inclusion of overshooting from the base of the outer convective zone during the pre-AGB phases on the surface abundances of the various chemical species will be discussed in the following sections.

2.3. Mass loss

Mass loss can be treated according to different prescriptions. It is possible to adopt the classic Reimers' treatment, the Vassiliadis & Wood (1993) formulation, or the prescription given by Blöcker (1995). In this latter case the strong increase of the mass loss rate during the AGB evolution is modeled by multiplying the Reimers' rate by an ad hoc luminosity power: the final expression is

$$\dot{M} = 4.83 \times 10^{-22} \eta_R M^{-3.1} L^{3.7} R \quad (2)$$

where η_R is the free parameter entering the Reimers' prescription. The Blöcker (1995) prescription was used to calculate all the models presented in this paper. The free parameter was chosen $\eta_R = 0.02$, according to the discussion in Sect. 3.

2.4. Nuclear network

The nuclear network includes 30 elements (up to ^{31}P) and 64 reactions. The full list of the 30 chemicals and of the reactions included can be found in Ventura & D'Antona (2005a).

The relevant cross section are taken from the NACRE compilation (Angulo et al. 1999) In the present work we test the effects of changing the following cross sections:

1. ^{14}N(p,γ)^{15}O (Formicola et al. 2004);
2. ^{22}Ne(p,γ)^{23}Na (Hale et al. 2002);
3. ^{23}Na(p,γ)^{24}Mg (Hale et al. 2004);
4. ^{23}Na(p,α)^{20}Ne (Hale et al. 2004).

In this work we focus on a chemistry that is typical of GCs, i.e. $Z = 0.001$, $Y = 0.24$. The initial abundances of all the elements are solar-scaled.

3. Oxygen vs. sodium abundances: the overall problem

The observed oxygen-sodium anticorrelation can be seen in Fig. 1, where we report the results of spectroscopic analysis of many giants in some of the GCs examined. We can clearly identify, for each cluster, a group of stars, in the right lower part of the diagram, with a "standard" chemical composition (i.e. [Na/Fe] = 0 and [O/Fe] = 0.3). In all clusters an additional population, which is oxygen-poor and sodium-rich, is also present: the sodium enhancement seems to saturate at Δ[Na/Fe] ∼ 0.6 dex even at the lowest oxygen abundances. The extent of this behaviour, and particularly the depletion of oxygen, is not homogeneous among the various clusters: we may fix a maximum value of Δ[O/Fe] ∼ 0.6–0.7 dex for the oxygen reduction, with the only exception of M 13, which exhibits a few stars for which the measured oxygen abundances are smaller than the standard by ∼1 dex (Sneden et al. 2004).

The abundances of sodium and oxygen undergo strong variations within a nuclearly active star, since both elements are involved in several reactions included in proton capture and He-burning nucleosynthesis.

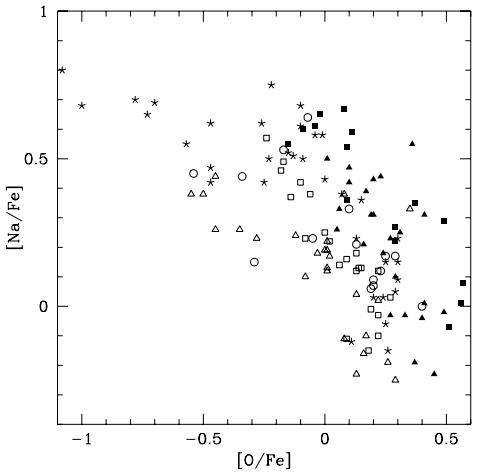

Fig. 1. The observed oxygen–sodium anticorrelation in GCs stars. The different symbols refer to the following clusters. Stars: M 13 (Sneden et al. 2004); open squares: M 3 (Sneden et al. 2004); full squares: NGC 6752 (Yong et al. 2005); full triangles: M 4 (Smith et al. 2005); open triangles: M 5 (Ivans et al. 2001); open circles: NGC 2808 (Carretta 2006). Typical errors are of the order of 0.1 dex.

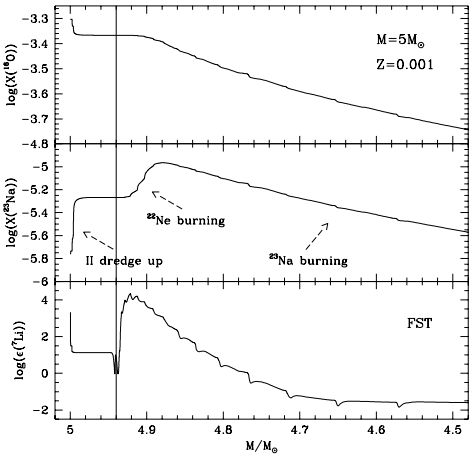

Fig. 2. The evolution in the early AGB phase of the surface abundances of oxygen (*top panel*), sodium (*middle*) and lithium (*bottom*) for a model of initial mass 5 $M_{\odot}$ with $Z = 0.001$.

Oxygen is essentially destroyed when the CNO cycle is active, a behaviour that is seen to be even more evident adopting the reduced cross sections of the ^{14}N(p,γ)^{15}O reaction (Formicola et al. 2004): this reaction acts as a bottleneck within the full CNO cycle, so that when the temperature is sufficiently high, oxygen burns, and is practically not recycled. On the other hand, oxygen is produced within the context of helium burning via the ^{12}C(α,γ)^{16}O reaction: in the stellar regions touched by 3α burning, the oxygen abundance is increased. In the intershell region, the oxygen abundance increases inwards from 2×10^{-6} to 10^{-5}.

Sodium is involved in proton capture reactions: it is produced via the ^{22}Ne(p,γ)^{23}Na channel, and is destroyed by two distinct modalities, i.e. via the two reactions ^{23}Na(p,γ)^{24}Mg and ^{23}Na(p,α)^{20}Ne. In the last few years the cross sections of all these 3 reactions were reconsidered and severely modified with respect to the NACRE prescription (Hale et al. 2002; 2004); this was a further motivation to perform the present exploration. Contrary to oxygen, it is not possible to establish a priori whether sodium is either produced or consumed when the above channels are efficiently activated: its abundance is in many contexts provided by an equilibrium value, thus depending also on the amount of ^{22}Ne available. Sodium is also indirectly touched by He-burning, because in this latter process the abundance of ^{22}Ne is considerably modified, as it is directly involved in some α captures.

On the basis of the above discussion, we understand that the surface abundances of the two elements during the AGB phase may change either because of HBB at the bottom of the surface convective zone, or by the effects of the third dredge-up (hereinafter TDU), which brings to the surface material precedently touched by helium burning.

Before proceeding with this discussion, it is important to note that the destruction of oxygen in AGB stars is found exclusively when an efficient treatment of convection (FST) is used. When the traditional MLT prescription is adopted, the temperatures at the bottom of the envelope never reach values compatible with an advanced nucleosynthesis, so that oxygen can be very hardly depleted at the surface. These results find a robust confirmation in all the AGB computations performed by various research groups (Fenner et al. 2004; Denissenkov & Herwig 2003).

Ventura & D'Antona (2005a) showed that the treatment of convection is by far the physical input having the largest impact on the results, on both the physical and chemical points of view: when the FST model is used, the models evolve at larger luminosities, hence larger mass loss rates, and consequently shorter evolutions. The number of TPs is drastically reduced, along with the number of TDU episodes: this has the effect of preventing that great amounts of CNO and ^{22}Ne rich material is transported to the external layers, and helps in keeping low both the C+N+O sum and the abundance of sodium.

Concerning the main target of the present study, i.e. the possibility of reproducing the oxygen vs. sodium anticorrelation, the massive AGB models calculated either with the FST or the MLT treatment of convection present opposite problems: the FST models can destroy oxygen easily, but at the same temperatures also deplete sodium, while the MLT models produce huge amounts of sodium (Fenner et al. 2004; Ventura & D'Antona 2005a) and also, via the TDU, maintain the oxygen content above the solar scaled value. We will therefore focus on the FST modeling of convection in the future steps of the present investigation[3]. We show in the two top panels of Fig. 2 the variation of the oxygen and sodium abundances at the surface of a model of initial mass $M = 5\ M_{\odot}$ during the AGB phase. We choose the mass as abscissa, to have also an idea of the chemical content of the material expelled by the star. We note on the left of both panels the effects of the second dredge-up, which increases the sodium and decreases the oxygen content of the envelope. Quantitatively, the results depend on the assumptions concerning the extra mixing assumed at the bottom of the convective zone, but we may limit the effects of the second dredge-up to an increase by at most ∼0.5 dex of sodium and a decrease by ∼0.1 dex of oxygen.

[3] It remains possible that a less efficient convection, of the MLT type, provides the required amount of oxygen depletion by HBB, e.g. in the envelopes of the more massive super-AGBs (Siess 2006), which then would be the only pollutors, acting on a timescale of 20–30 Myr after the birth of the first stellar generation. The problem of cross sections discussed in this paper remains similar, although the environment for the elements nucleosynthesis will be different. Notice that, if super-AGBs are the main pollutors, the IMF problem becomes worse.

At the very beginning of the Thermal Pulses phase, the temperatures at the bottom of the envelope do not allow an advanced nucleosynthesis beyond the CN cycle, which is confirmed by the flat profiles of all the abundances shown in the three panels of Fig. 2 for $M > 4.95\ M_{\odot}$. The thin vertical lines mark approximately the beginning of the lithium production via the Cameron & Fowler (1971) mechanism, which requires temperatures of the order of $T \sim 40 \times 10^6$ K. Slightly later, the ^{22}Ne nuclei previously dredged-up undergo proton capture to produce ^{23}Na, whose surface abundance increases. This production of sodium is accompanied by a depletion of oxygen, confirming that full CNO cycling operates at the bottom of the surface convective zone: this is the only phase during the whole AGB evolution when the surface oxygen and sodium show an opposite behaviour. This trend is reversed when the ^{22}Ne content within the envelope becomes so low that the rate of sodium destruction exceeds the production: the surface abundance of sodium, after an increase of ∼1 dex compared to initial solar scaled value, starts to decrease (see the middle panel of Fig. 2).

By examining the central panel of Fig. 2, we also might expect that the average sodium content of the ejecta depends on the mass loss rate adopted. Ventura & D'Antona (2005b) discussed the possibility that increasing the mass loss rate would "expand" (in mass) the phase when the abundance of sodium is still very high, with the consequent increase of the yield: yet, we may see from the top panel that this would also have the effect of stretching the phase when the oxygen abundance is still large, which would be of little help in the attempt of reproducing the low oxygen abundances observed in the GCs stars samples so far examined.

Also, a larger mass loss rate would have a dramatic effect on the abundance of lithium, and its yield would be not consistent with the observations: a mass loss rate much larger or smaller than what comes out by our assumption of $\eta = 0.02$, in Eq. (2) is not compatible with the observed abundances of lithium in metal-poor GCs (values of $\log N(\mathrm{Li}) = 2.1$–$2.3$ are determined in NGC 6397 by Bonifacio et al. 2002, and values $\log N(\mathrm{Li}) = 2.0$–$2.3$ in NGC 6752 by Pasquini et al. 2005). E.g. we have shown that the lithium abundance obtained by models in which $\eta = 10$ are too large ($\log N(\mathrm{Li}) \sim 3$, Ventura et al. 2002). This is a consequence of the fact that the lithium abundance in the envelope during the production phase is very high, but it drops to insignificant abundances when all the ^{3}He is consumed. Consequently, the exact mass loss rate during the phase of lithium production determines the lithium yield much more severely than the other important yields, such as the CNO or sodium.

This latter consideration, along with a precedent calibration of the mass loss rate during the AGB phase based on the luminosity function of lithium rich AGBs observed in the Magellanic Clouds presented by Ventura et al. (2000), is the motivation behind our choice of restricting our attention on the standard rate used by Ventura & D'Antona (2005a–c), i.e. the Blöcker prescription with $\eta = 0.02$.

4. The standard overall evolution of a 5 $M_{\odot}$ model

All the models discussed below have an initial mass $M = 5\ M_{\odot}$. Proton capture by ^{14}N nuclei was described using the new cross sections by Formicola et al. (2004). The differences on the stellar structure with respect to models calculated with the NACRE rates are discussed below.

4.1. The pre-AGB evolution

During the main sequence (MS) phase, the star develops a CNO burning core, which reaches a maximum extension of ∼1.5 $M_{\odot}$. The total duration of the H-burning phase is $\tau_{\mathrm{H}} = 90$ Myr. During the first dredge-up, the surface convection penetrates inwards, reaching a layer 2.1 $M_{\odot}$ away from the centre: during this phase the only changes in the surface chemistry involve lithium (whose abundance drops from $\log(\epsilon(^7\mathrm{Li})) = 3.3$ to $\log(\epsilon(^7\mathrm{Li})) = 1.5$), carbon (whose mass fraction decreases from the initial $X(^{12}\mathrm{C}) = 1.73 \times 10^{-4}$ to 1.26×10^{-4}) and nitrogen (which increases from $X(^{14}\mathrm{N}) = 5.1 \times 10^{-5}$ to 1.2×10^{-4}).

The duration of the He-burning phase is $\tau_{\mathrm{He}} = 12$ Myr. The extension of the convective core while the 3α reactions are active is ∼0.5 $M_{\odot}$. After the exhaustion of the core helium, a rapid expansion of the whole external layers extinguishes the CNO burning shell, and the surface convection penetrates inwards, reaching a layer at a mass distance from the centre of ∼0.93 $M_{\odot}$. This will be the core mass of the star at the beginning of the following AGB evolution. Also in this case the surface abundances of lithium, carbon and nitrogen, change: lithium drops to $\log(\epsilon(^7\mathrm{Li})) = 1.1$, carbon to $X(^{12}\mathrm{C}) = 1.11 \times 10^{-4}$, while nitrogen increases to $X(^{14}\mathrm{N}) = 1.8 \times 10^{-4}$. In addition, $X(^{16}\mathrm{O})$ is reduced from the initial solar scaled value of $\sim 5 \times 10^{-4}$ to 4.3×10^{-4}; the sodium content rises from $X(^{23}\mathrm{Na}) = 1.7 \times 10^{-6}$ to 5.4×10^{-6}. Finally, we see a considerable increase of the helium mass fraction, which rises to $Y = 0.31$; when extra mixing during the second dredge-up is considered, the final helium abundances found is $Y = 0.33$, which is quite close to the helium content invoked by D'Antona & Caloi (2004) to explain the morphology of the horizontal branch (HB) of the cluster NGC 2808.

As expected, the total duration of the pre-AGB phase is very short (∼100 Myr) compared to the age of GCs.

4.2. The AGB phase

We consider as "standard" the AGB evolution calculated with no extra mixing from the bottom of the convective envelope.

The model evolves at large luminosities since the early AGB phase, due to the rapid increase of the temperature at the base of the convective envelope (hereinafter T_{bce}) since the first TPs: after the third TP, $T_{\mathrm{bce}} \sim 90 \times 10^6$ K during the quiescent CNO burning phase. The total number of TPs experienced by the star is 30, spread over a global duration of the AGB phase of $\tau_{\mathrm{AGB}} = 90\,000$ yr. During this time the core mass grows by 0.025 $M_{\odot}$, reaching a final value of $M_{\mathrm{core}} \sim 0.96\ M_{\odot}$. The luminosity increases until the 21th after pulse, when the envelope mass is reduced to 2 $M_{\odot}$, slowly declining afterwards; a similar behaviour is shown by T_{bce}, which reaches a maximum of $T_{\mathrm{bce}} = 106 \times 10^6$ K in conjunction with the maximum luminosity. We note that with the only exceptions of the first and the very latest TPs, T_{bce} keeps approximately constant during the whole AGB evolution: this allows us to use the same value to evaluate the time scales of the reactions involved, on the basis of their cross sections at this temperature.

The Cameron Fowler mechanism is activated at the very beginning of the AGB phase: the star attains surface large lithium abundances (i.e. $\log(\epsilon(^7\mathrm{Li})) = 2$) already after the second TP. The lithium rich phase lasts until the 9th pulse, after which the surface abundance of lithium declines rapidly to its final equilibrium value of $\log(\epsilon(^7\mathrm{Li})) \sim -2$.

The TDU is found after 19 TPs; its maximum efficiency, reached asymptotically, is $\lambda = 0.3$. The large degree of CNO nucleosynthesis can be seen in Fig. 3, where we report the

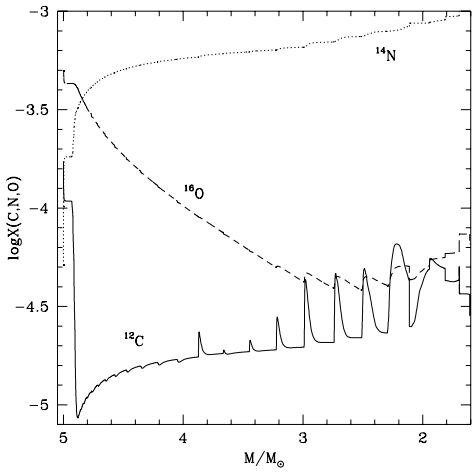

Fig. 3. The variation with mass of the abundances of the CNO elements at the surface of the same model of Fig. 2. The sudden increase of the mass fraction of carbon is a clear signature of the TDU.

variation with mass of the surface abundances of CNO. We note in particular the strong depletion of oxygen, which reaches a minimum value of $X(^{16}\mathrm{O}) = 4 \times 10^{-5}$ (a factor of 10 lower than the starting abundance) before the TDU prevents further depletion. This result confirms that strong oxygen depletion is naturally achieved when an efficient treatment of convection is used during the AGB phase.

4.3. The role of the ^{14}N(p,γ)^{15}O cross section

Recently, within the context of the LUNA collaboration, the ^{14}N(p,γ)^{15}O reaction of the CNO cycle has been re-determined (Formicola et al. 2004). Weiss et al. (2005) examined the changes introduced by the new rates in many cases of interest for stellar astrophysics, ranging from low mass stars evolution (both on the MS and HB) to intermediate mass models of solar metallicity. We explore here models with the same mass as those calculated by Weiss et al. (2005), with the only difference that we adopt a metallicity $Z = 0.001$.

During the core H-burning phase we find qualitatively the same differences found by Weiss et al. (2005): the track calculated with the new rates is sligthly hotter, and the whole MS life-time is $\sim 5 \times 10^5$ yr shorter (to be compared to a difference of ∼1 Myr found by Weiss et al. 2005). The extension of the blue loops during the core He-burning phase is similar in the two cases.

Turning to the AGB phase, when using the new rates we find, in agreement with Weiss et al. (2005), larger 3α peak luminosities at each TP, and a slightly larger luminosity even during the quiescent CNO burning phase. For that concerning the surface oxygen abundance, the new rates favour a larger depletion, the minimum value (reached before TDU starts and increases the oxygen content of the envelope after each TP) being $X(^{16}\mathrm{O}) = 4 \times 10^{-5}$, compared to $X(^{16}\mathrm{O}) = 7 \times 10^{-5}$ found when using the NACRE rates.

5. The surface abundances of oxygen and sodium

The cross sections of the reactions involving sodium (i.e. the proton capture by ^{22}Ne nuclei and the two proton capture reactions by sodium itself) were recently revised by Hale et al. (2002) and Hale et al. (2004). Compared to the NACRE compilation, on which all the previous works on this topic by Ventura & D'Antona (2005a–c) were based, the recommended rates present the following differences:

1. Based on a reduction of the 151-KeV resonance strength, the rate of the ^{22}Ne(p,γ)^{23}Na reaction is significantly smaller than the NACRE value: at the temperatures of interest in the present work, i.e. $T \sim 10^8$ K, we find a maximum difference of 3 dex (see Fig. 10 in Hale et al. 2002).
2. The rate of the (p, γ) capture reaction by ^{23}Na nuclei was also significantly reduced (by a factor of ∼30) compared to NACRE. A smaller reduction factor is found for the (p, α) channel.
3. Compared to the NACRE prescrition, the new rates favour the Ne-Na cycle, because of the high $\langle \sigma v \rangle_{(p,\alpha)} / \langle \sigma v \rangle_{(p,\gamma)}$ ratio.

The three points above must be taken with some caution, considering the large uncertainties associated with any single reaction rates. As an example, for point (2) above, the uncertainties on the reaction reates of the two proton captures by sodium nuclei at the temperatures of interest here are ∼4 dex and ∼1 dex, respectively, for the (p, γ) and (p, α) channels. As for point (3), the more recent experiments carried by Rowland et al. (2004) confirm that at $T \sim 10^8$ K the NeNa cycle is almost closed, but the amount of matter escaping from the cycle, determined by the $(p, \gamma)/(p, \alpha)$ ratio, is still highly uncertain, as it is confirmed by looking at Fig. 1 by Rowland et al. (2004).

With these cautions in mind, we analyse the evolution of the surface abundance of sodium within our models.

First, we note that use of the recommended rates for the proton capture by ^{22}Ne nuclei is not compatible with any sodium production, because the relevant cross section is so low that the nucleosynthesis would be displaced towards ^{22}Ne. In other words, sodium would be destroyed by the (p, α) reaction, with a consequent increase of the two neon isotopes abundances, and with a negligible feedback on the sodium content. This led us to use in all the models presented here the upper limits of the ^{22}Ne$(p, \gamma)^{23}$Na reaction rates provided by Hale et al. (2002), which, at the temperatures of interest here, are very similar (actually slightly larger) than those recommended by NACRE.

At the beginning of the AGB phase, as a result of the second dredge-up, the abundances of the two neon isotopes and of sodium are $X(^{20}\mathrm{Ne}) = 8 \times 10^{-5}$, $X(^{22}\mathrm{Ne}) = 5.7 \times 10^{-6}$ and $X(^{23}\mathrm{Na}) = 5.5 \times 10^{-6}$. These values differ considerably from the equilibrium values $X(^{22}\mathrm{Ne})/X(^{20}\mathrm{Ne}) = 5 \times 10^{-4}$, and $X(^{23}\mathrm{Na})/X(^{22}\mathrm{Ne}) = 17$ expected on the basis of the cross sections used in this work, i.e. the lower limit provided by Hale et al. (2002) for the ^{22}Ne$(p, \gamma)^{23}$Na reaction, and the recommended values by Hale et al. (2004) for the proton captures by ^{23}Na nuclei. The ^{22}Ne in excess is burnt, and the equilibrium abundances are reached after 15 TPs, when the total stellar mass is reduced to 4 $M_\odot$. The remaining AGB phase, with the only exception of the latest TPs when the TDU begins, will be at approximately the equilibrium abundances, i.e. $X(^{20}\mathrm{Ne}) = 9.1 \times 10^{-5}$, $X(^{22}\mathrm{Ne}) = 5 \times 10^{-8}$ and $X(^{23}\mathrm{Na}) = 8 \times 10^{-7}$.

The equilibrium abundance of sodium is therefore a factor of ∼2 lower compared to the initial solar scaled abundance: this counterbalances the initial production phase, so that the global yield of sodium turns out to be $[^{23}\mathrm{Na/Fe}] = 0$. Turning our attention to the oxygen-sodium anticorrelation, we must combine this result with the oxygen content of the ejecta, which, after scaling by 0.3 dex to account for the initial α enhancement, is $[^{16}\mathrm{O/Fe}] = -0.4$. Looking at Fig. 4, we note that the theoretical point (corresponding to the full square with the lowest [Na/Fe]) would be in the central lower part of the [O-Na] plane, a region indeed not covered by any observed star.

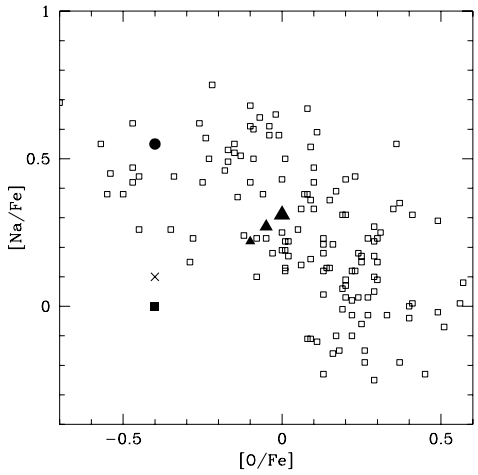

Fig. 4. The theoretical yields of the models compared to the observed abundances in GCs stars (open squares). The three big points on the left (full square, cross, and full circle) represent the yields of the models calculated without extra mixing, with different assumptions concerning the cross sections of the main channel for sodium destruction, i.e. the (p, α) reaction (see text for details). The full triangles represent the ejecta of the models calculated with extra mixing (the dimensions of the triangles are indicative of the extension of the extra-mixing zone).

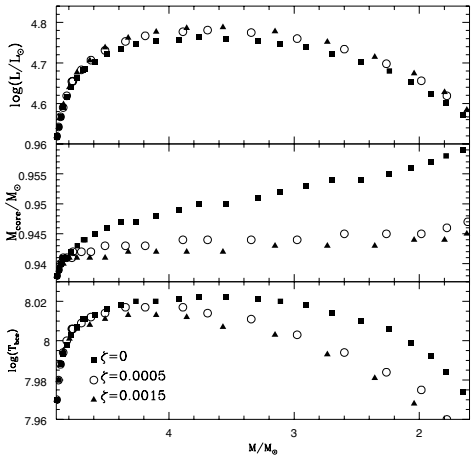

Fig. 5. The variation with mass of the main physical properties of three AGB models of initial mass 5 $M_{\odot}$ calculated with different values of the extra-mixing parameter ζ.

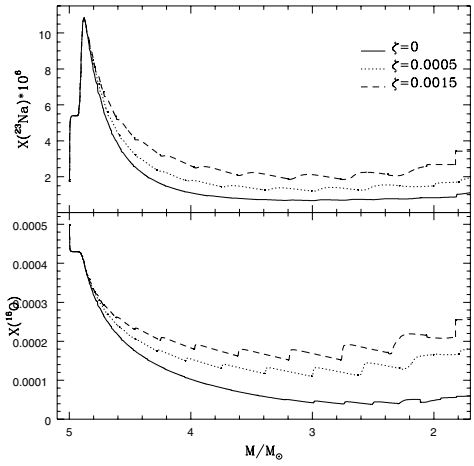

Fig. 6. The effects of the extra-mixing parameter ζ on the surface abundances of sodium (*top*) and oxygen (*bottom*).

5.1. The effects of extra mixing

If the convective velocities are assumed not to vanish abruptly at the bottom of the convective envelope, but rather to decay exponentially, some extra mixing occurs, which facilitates the occurrence of the TDU, and consequently brings some CNO rich material, as well as some fresh ^{22}Ne, to the surface: since ^{22}Ne is easily converted into ^{23}Na by proton capture when the temperature is sufficiently high, we expect that the sodium yield is increased if we assume $\zeta > 0$.

Ventura & D'Antona (2005c) made a first qualitative exploration on this issue, showing that a modest extra mixing could indeed raise the abundance of sodium, by the mechanism described above. In that work extra mixing was included only in the latest evolutionary phases, when TDU had already been found within the star. We follow a more systematic approach here.

We therefore calculated various AGB evolutions with all the same input physics, differing only for the values of ζ. We first checked which value of ζ would make the total C+N+O content of the ejecta to exceed by a factor of 2 the initial sum: ζ cannot exceed this value, as even the most anomalous stars show up only a modest increase of the C+N+O (Ivans et al. 1999), by at most a factor of 2. We find that all the models with $\zeta \leq 0.0015$ meet this request. This range of values for ζ leads to a very modest extension of the extra-mixing zone, as we may understand from a comparison with the values of ζ calibrated in Ventura et al. (1998) to fit the main sequences of open clusters, which was $0.02 \leq \zeta \leq 0.03$. The mass involved in the extra-mixing region is of the order of $\Delta M \sim 10^{-6}\ M_{\odot}$.

First, we note that the assumption of some extra mixing determines some changes on the physical evolution of the model. Figure 5 compares the variation with mass of the physical properties of some models calculated with different ζ values. The models with the larger ζ evolve at lower core masses (hence, lower temperatures at the bottom of the convective zone), but at higher luminosities, because of the fresh CNO products brought at the surface by each TDU; this also determines a smaller number of TPs, because of the larger mass loss triggered by this extra luminosity (in other words, the "distance in mass" between two following TPs increases with ζ).

In all the models calculated with extra-mixing, independently of ζ, a ^{13}C pocket is formed following each TP, when the convective envelope penetrates inwards.

The two panels of Fig. 6 show the effects of ζ on the yields of sodium and oxygen: as expected, the sodium content of the ejecta is larger for larger ζ's, but also the oxygen abundance increases, because it is dredged-up more easily when some extra mixing is used.

In the [O-Na] plane, we see from Fig. 4 that the models calculated with overshooting (represented as full triangles) occupy a region of the diagram where we find stars having a moderate depletion of oxygen (~0.3 dex) and enhancement of sodium (~0.3 dex).

These results seem consistent with the observations. Nevertheless, we still are not able to reproduce the low oxygen – high sodium observations.

5.2. The role of cross sections

We calculated an evolutionary sequence starting from the same model at the beginning of the AGB phase, taking the lower limits provided by Hale et al. (2004) for the main channel of sodium

destruction, i.e. the (p, α) reaction; we still use the upper limit provided by Hale et al. (2002) for proton capture by ^{22}Ne. The result, i.e. [^{23}Na/Fe] = 0.1, is consistent with the previous discussion based on the equilibrium abundances, because the lower limit of the rates presented by Hale et al. (2004) is 0.1 dex smaller than the recommended value, at the relevant temperatures; we represent the corresponding theoretical yields with a cross in Fig. 4.

Only if we assume that the cross sections of the ^{23}Na(p,α)^{20}Ne reaction by sodium nuclei is smaller by a factor of ∼4 than the recommended value we can reconcile quantitatively the theoretical yields with the observed abundances: in this case the theoretical point, represented in Fig. 4 as a full circle, would shift upwards to ([O/Fe], [Na/Fe]) = (−0.4, 0.6), which would be consistent with the O-Na relation defined by the stars observed in GCs with the most anomalous and extreme chemistry[4].

If we take into account the very probable α-enhancement of ^{20}Ne, *we need a cross section of the above reaction only a factor ∼2 smaller than the recommended value*. In fact, as already discussed at the beginning of this section, the Hale cross sections (supported by the Rowland et al. (2004) work) favour an almost constant sum S of the abundances of the two neon isotopes and of sodium, so that, at equilibrium, X(^{23}Na) ∝ S. Since, even in the solar case, ^{20}Ne accounts for almost the 90% of S, it is straightforward that an increase of the ^{20}Ne abundance by 0.3 dex (as expected because of $\alpha-$enhancement) almost doubles the final sodium equilibrium abundance, so that, with the recommended cross sections, we find [^{23}Na/Fe] = 0.25. Assuming a cross section for the ^{23}Na$(p, \alpha)^{20}$Ne reaction diminished by a factor of two would lead to an average chemical composition of the ejecta ([O/Fe], [Na/Fe]) = (−0.4, 0.55), again consistent with the abundances of oxygen and sodium measured in the stars of the sample evidentiating the strongest depletion of ^{16}O; since the lower limit of the (p, α) rate is only 0.1 dex smaller than the recommended value, the lowering by a factor of 2 needed here cannot be merely statistical, but rather due to unknown systematic uncertainties.

6. Conclusions

In this paper we discuss the possibility that massive AGBs ejecta provide a chemical composition in agreement with the oxygen-sodium anticorrelation observed in giant and TO stars belonging to GCs.

A clear result of the present work is that a high sodium content of the ejecta of these stars can be obtained only if the upper limits provided by Hale et al. (2002) for the rates of the reaction ^{22}Ne(p,γ)^{23}Na are used; when the recommended cross sections are adopted, the ejecta would be neon rich but sodium poor.

We tested the effects of including some extra mixing from the bottom of the surface convective zone. We fixed an upper limit to ζ, the overshooting parameter, by demanding that the total C+N+O content of the ejecta is not increased by more than a factor of 2: this leads to $\zeta \leq 0.0015$, a value much smaller than that used for simulating overshooting from convective cores during the major phases of nuclear burning. Even a modest amount of extra mixing increases the sodium content of the ejecta via dredge-up of ^{22}Ne, but it also increases the oxygen mass fraction. In this case the ejecta would show up a mild depletion of oxygen and depletion of sodium, and would well correspond to the chemical content of the stars showing the intermediate chemical composition. This would leave open the issue of reproducing the most extremely anomalous group of stars present in all the GCs examined.

The standard models calculated with no extra mixing from the base of the envelope destroy oxygen very easily, altough their sodium yield is considerably lower than that indicated from the observations; this conclusion holds even when the lower limits of the cross sections of the main channel of sodium destruction are used. The theoretical yields may be reconciled with the observations only if we assume that the cross section of the main channel of sodium destruction is a factor of ∼2 below the recommended rates. In this case, the ejecta of these objects would reproduce the abundances of the stars with the most anomalous chemical composition, i.e. those showing up the largest extent of sodium enhancement and oxygen depletion; the group of stars showing only a mild depletion of oxygen would correspond to the ejecta of less massive models (i.e. $M \sim 4\ M_{\odot}$), which have lower temperatures at the bottom of the convective envelope.

It is also possible that the main pollution of the cluster gas is the matter expelled from the stars we are considering here, which have the maximum oxygen depletion and sodium enrichment. In this case, the milder compositions in Na and O correspond to dilution of this matter into different amounts of pristine remnant cluster gas.

[4] With the only exception of M 13.

References

Angulo, C., Arnould, M., Rayet, M., et al. 1999, Nucl. Phys. A, 656, 3
Blöcker, T. 1995, A&A, 297, 727
Blöcker, T., & Schönberner, D. 1991, A&A, 244, L43
Bonifacio, P., Pasquini, L., Spite, M., et al. 2002, A&A, 390, 91
Canuto, V. M. C., & Mazzitelli, I. 1991, ApJ, 370, 295
Canuto, V. M. C., Goldman, I., & Mazzitelli, I. 1991, ApJ, 473, 550
Carretta, E. 2006, AJ, 131, 1766
Cloutman, L., & Eoll, J. G. 1976, ApJ, 206, 548
Cottrell, P. L., & Da Costa, G. S. 1981, ApJ, 245, L79
D'Antona, F., & Caloi, V. 2004, ApJ, 611, 871
D'Antona, F., Bellazzini, M., Caloi, V., et al. 2005, ApJ, 631, 868
Denissenkov, P., & Herwig, F. 2003, ApJ, 590, L99
Fenner, Y., Campbell, S., Karakas, A. I., Lattanzio, J. C., & Gibson, B. K. 2004, MNRAS, 353, 789
Formicola, A., Imbriani, G., Costantini, H., et al. 2004, Phys. Lett. B, 591, 61
Gratton, R., Sneden, C., & Carretta, E. 2004, ARA&A, 42, 385
Hale, S. E., Champagne, A. E., Iliadis, C., et al. 2002, Phys. Rev. C, 65, 5801
Hale, S. E., Champagne, A. E., Iliadis, C., et al. 2004, Phys. Rev. C, 70, 5802
Ivans, I. I., Sneden, C., Kraft, R. P., et al. 1999, AJ, 118, 1273
Ivans, I. I., Kraft, R. P., Sneden, C., et al. 2001, AJ, 122, 1438
Pasquini, L., Bonifacio, P., Molaro, P., et al. 2005, A&A, 441, 549
Piotto, G., et al. 2005, ApJ, 621, 777
Rowland, C., Iliadis, C., Champagne, A. E., et al. 2004, ApJ, 615, L37
Siess, L. 2006, A&A, 448, 717
Smith, V. V., Cunha, K., Ivans, I. I., et al. 2005, ApJ, 633, 392
Sneden, C., Kraft, R. P., Guhathakurta, P., Peterson, R. C., & Fulbright, J. P. 2004, AJ, 127, 2162
Vassiliadis, E., & Wood, P. R. 1993, ApJ, 413, 641
Ventura, P., & D'Antona, F. 2005a, A&A, 431, 279
Ventura, P., & D'Antona, F. 2005b, A&A, 439, 1075
Ventura, P., & D'Antona, F. 2005c, ApJ, 635, L149
Ventura, P., Zeppieri, A., D'Antona, F., & Mazzitelli, I. 1998, A&A, 334, 953
Ventura, P., D'Antona, F., Mazzitelli, I., & Gratton, R. 2001, ApJ, 550, L65
Ventura, P., D'Antona, F., & Mazzitelli, I. 2002, A&A, 393, 215
Vitense, E. 1953, Zs.Ap., 32, 135
Weiss, A., Serenelli, A., Kitsikis, A., Schlattl, H., & Christensen-Dalsgaard, J. 2005, A&A, 441, 1129
Yong, D., Lambert, D. L., & Ivans, I. I. 2003, ApJ, 599, 1357
Yong, D., Grundahl, F., Nissen, P. E., Jensen, H. R., & Lambert, D. L. 2005, A&A, 438, 875
Yong, D., Aoki, W., & Lambert, D. L. 2006, ApJ, 638, 1018